Franck–Condon simulation of the A 1 B 2 X 1 A 1 dispersed fluorescence spectrum of fluorobenzene and its rate of the internal conversion

Rongxing He, Ling Yang, Chaoyuan Zhu, Masahiro Yamaki, Yuan-Pern Lee, and Sheng Hsien Lin

Citation: The Journal of Chemical Physics **134**, 094313 (2011); doi: 10.1063/1.3559454
View online: http://dx.doi.org/10.1063/1.3559454
View Table of Contents: http://scitation.aip.org/content/aip/journal/jcp/134/9?ver=pdfcov
Published by the AIP Publishing

Franck–Condon simulation of the $A\ ^1B_2 \rightarrow X\ ^1A_1$ dispersed fluorescence spectrum of fluorobenzene and its rate of the internal conversion

Rongxing He,[1,2] Ling Yang,[1,3] Chaoyuan Zhu,[1,a)] Masahiro Yamaki,[4] Yuan-Pern Lee,[1] and Sheng Hsien Lin[1,4]

[1]*Department of Applied Chemistry, Institute of Molecular Science and Center for Interdisciplinary Molecular Science, National Chiao-Tung University, Hsinchu 30050, Taiwan*
[2]*College of Chemistry and Chemical Engineering, Southwest University, Chongqing 400715, China*
[3]*Department of Chemistry, Beijing Normal University, Beijing 100875, People's Republic of China*
[4]*Institute of Atomic and Molecular Sciences, Academia Sinica, Taipei 106, Taiwan*

(Received 16 August 2010; accepted 7 February 2011; published online 7 March 2011)

By using three different hybrid exchange-correlation functionals containing 20%, 35%, and 50% of exact Hartree–Fock (HF) exchange of the density functional theory and its time-dependent extension plus the Hartree–Fock and the configuration interaction of single excitation methods, equilibrium geometries, and their 30 vibrational–normal-mode frequencies of the ground $S_0(^1A_1)$ and the first excited $S_1(^1B_2)$ states of fluorobenzene (FB) were calculated. The dispersed fluorescence spectrum and internal conversion (IC) rate of the $A\ ^1B_2 \rightarrow X\ ^1A_1$ transition were simulated by Franck–Condon (FC) calculations within the displaced harmonic oscillator approximation plus anharmonic and distorted corrections. The simulated spectral profile is primarily described by the Franck–Condon progression from the ring-breathing modes ν_9 and ν_{10} which belong to totally symmetry modes. Anharmonic corrections simultaneously improve the intensity order of 9_1^0 and 10_1^0 bands and diminish 1_1^0 transition that is fairly strong in harmonic simulations. It is concluded that the amount of Hartree–Fock exchange does impact the geometries and vibrational frequencies of FB molecule, but not the relative intensities of the transitions. It is anharmonic corrections that make the relative intensities of the transitions in good agreement with experimental results. Distorted corrections could assign most of the dominant overtones of out-of-plane nontotally symmetry modes, and the results agree well with the experimental assignments. Furthermore, it was found that the internal conversion rate is dominated by three promoting modes that are computed with lowing symmetry to C_1. By choosing dephasing width as 10 cm^{-1} that is consistent with spectral simulation, we obtained the lifetimes of the $A\ ^1B_2 \rightarrow X\ ^1A_1$ de-excitation as 11 and 19 ns, respectively, from TD(B3LYP) and HF/CIS calculations in comparison with the experimental value 14.75 ns. © *2011 American Institute of Physics*. [doi:10.1063/1.3559454]

I. INTRODUCTION

Fluorobenzene (FB) molecule is the simplest prototypical benzene derivative and the study of its spectroscopic and photophysical properties has a long history with focusing on its electronic ground $[S_0(^1A_1)]$ and first singlet excited $[S_1(^1B_2)]$ states.[1–5] The presence of fluorine atom on aromatic ring reduces the D_{6h} point group symmetry of benzene to the C_{2v} symmetry of FB and this makes the electronic structures and spectroscopic characteristics of FB very different from those of benzene.[6–8] Therefore, it has been an interesting subject for both experimental and theoretical investigation of vibrational assignments from its absorption and fluorescence spectra.[1–10] As early as 1925, Henri had studied the near ultraviolet absorption spectrum of FB, and later in 1945 Wolman remeasured this spectrum with more details and found that strong perturbation of aromatic ring by fluorine atom enhances the transitions originally forbidden in benzene but permitted in FB.[11] In order to assign vibrational and electronic transitions in terms of vibronic levels, a few experiments with the high resolution of infrared vibrational and electronic absorption spectra of FB have been performed.[2–5,8–10,12] Lipp and Seliskar obtained the most complete assignment of the $S_1(^1B_2) \leftarrow S_0(^1A_1)$ excitation spectrum experimentally using the hot and cool band spectra.[2,3] Padma and Jug[13] calculated the equilibrium geometries of electronic ground and first excited states, and adiabatic excitation energy between the two electronic states using configuration interaction (CI) and semiempirical methods. Fogarasi and Császár[14] simulated the vibrational spectrum of the ground state using Hartree–Fock method. More recently, Miura *et al.*[15] computed the vertical excitation energy and oscillator strength of the $^1B_2 \leftarrow {}^1A_1$ transition of FB (corresponding to $^1E_{1u} \leftarrow {}^1A_{1g}$ transition in benzene) by the time-dependent density functional theory (TDDFT). Using more sophisticated experimental measurements of laser-induced fluorescence (LIF) and dispersed fluorescence (DF) spectroscopy, Butler *et al.*[4] provided almost complete assignment and interpretation of this cold band $^1B_2 \leftarrow {}^1A_1$ transitions of FB, and furthermore they analyzed over 40 single vibronic levels of DF spectra

a)Electronic mail: cyzhu@mail.nctu.edu.tw.

resulted in the assignment of 16 fundamental frequencies in the excited electronic state. Using the gas phase resonance enhanced multiphoton ionization (REMPI) technique and zero electron kinetic energy spectroscopy, Pugliesi *et al.*[5] could refine the assignments of the lower wavenumber region (below $\sim$1000 cm^{-1}) of the band $^1B_2 \leftarrow {}^1A_1$ transitions of FB. The Duschinsky effect (mode mixing) that was analyzed by high level *ab initio* calculations leaded to assignments of the considerable weak transitions observed in experiment spectrum[4,5] and relative intensities of the two-color (1 + 1′) REMPI spectrum of FB were simulated by performing numerical multidimensional Franck–Condon (FC) calculations including standard linear Duschinsky normal coordinate transformation procedure.[5]

A main purpose of the present work focuses on the *ab initio* simulations of electronic spectra and internal conversion (IC) of Fluorbenzene. From theoretical point of view, these two processes are partly governed by the same Franck–Condon factor. In order to demonstrate how accurate simulation we can do for internal conversion process, we must show that the same *ab initio* level of calculation should perform well for electronic spectra. Time dependent density function method is used to calculate excited state in which the impact of Hartree–Fock exchange percentage in the hybrid functional is extensively investigated and discussed.

In the present work, we first simulated the dispersed fluorescence electronic spectrum of FB following LIF excitation of the $^1B_2 \leftarrow {}^1A_1$ by employing simple products of one-dimensional FC factors that corresponds to displaced harmonic oscillator approximation plus anharmonic and distorted effects. We believe that the DF spectral profile should be primarily described by the Franck–Condon progression in terms of the totally symmetry normal modes. Anharmonic correction to ground and excited states is assumed to be the same and thus their corrections are only to totally symmetry normal modes. The distorted effects that affect only nontotally symmetry normal modes should be small as it can be considered as diagonal-part correction of Duschinsky mode-mixing matrix. We calculated the internal conversion rate of FB molecule following excitation of the $^1B_2 \leftarrow {}^1A_1$ transition under the isolated molecular condition. Actually, the lifetimes and the radiationless transition rates from the single vibronic levels of S_1 state were measured under the collision-free condition by Abramson and co-workers.[16,17] Reported lifetimes and quantum yields of fluorescence come from 59 vibronic states, and the lifetime of 0–0 transition is about 14.8 ns.[16] Radiationless transition involving two electronic states is partly governed by the nonadiabatic coupling that is determined by the off-diagonal matrix elements of the nuclear kinetic operators. This nonadiabatic coupling can be expressed in terms of series of normal-mode vibronic couplings which can be calculated by *ab initio* quantum mechanic methods and rate of internal conversion is usually sensitive to accuracy of those vibronic couplings.

The present paper is organized as follows. Section II describes computational details for applying *ab initio* methods to electronic structure, and for applying displaced oscillator approximation of FC factors to DF spectrum and IC rate constant. Section III presents the results and discussions and Sec. IV provides concluding remarks.

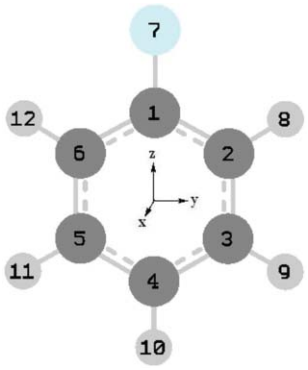

FIG. 1. The molecular structure and the atom numbering of fluorobenzene.

II. COMPUTATIONAL METHODS

A. *Ab initio* methods for electronic properties

It is important to notice that for molecule belonging to the C_{2v} point group symmetry the choice of B_1 and B_2 irreducible representations of electronic states depends on choice of Cartesian axes. Typically, the molecular C_2 axis is chosen as the z-axis and then the molecule is placed in the yz-plane with x-axis to be perpendicular to the molecular plane as shown in Fig. 1. In this way, we can identify the first excited state as B_2 symmetry.

The equilibrium geometries and its 30 vibrational frequencies of FB molecule were calculated in the framework of the density functional theory (DFT) for electronic ground state S_0 and time-dependent density functional theory for the first excited state S_1. We have reported calculations based on three kinds of different exchange-correlation functionals. The Becke's three-parameter hybrid functional with the Lee–Yang–Parr correlation functional (B3LYP)[18–21] was chosen as preliminary functional. Guthmuller and Champagne[22] pointed out that the percentage of Hartree–Fock (HF) exchange in the hybrid functionals has great impact. Therefore, we followed their choice with adding the other two hybrid functionals, BHandHLYP and B3LYP-35 (see Ref. 22 for definition) containing 50% and 35% HF exchange in comparison with 20% in B3LYP functional. We have also done the Hartree–Fock calculation in comparison with DFT for the ground state S_0 and the configuration interaction of single (CIS) excitation calculation in comparison with TDDFT for the excited state S_1. All the DFT, TDDFT, HF, and CIS calculations were carried out using GAUSSIAN 09 program[23] with basis set 6-311++G**. In the Franck–Condon simulation of the DF spectrum, the geometrical parameters and frequencies should be used consistently at the same level of *ab initio* methods, that is, DFT versus TDDFT and HF versus CIS, for the ground and the excited states, respectively.

For computing the IC rate constant of the $S_1(^1B_2) \rightarrow S_0(^1A_1)$ decay processes, we utilized the CASSCF/6-

311++G** level to evaluate the electronic nonadiabatic coupling matrix (vibronic couplings) between the S_0 and S_1 states. This was carried out using MOLPRO program.[24]

B. Franck–Condon simulation for DF spectra

The relative intensity of molecular fluorescence is theoretically proportional to the third power of frequency spectrum ω, but when it is converted into units used in experimental measurement, the intensity must be divided by ω^2.[25] Therefore, within the Born–Oppenheimer approximation, fluorescence coefficient $I(\omega)$ of the electronic transition from the initial state a to the final state b with vibrational quanta v and v', respectively, can be expressed as[26–28]

$$I(\omega) = \frac{4\pi^2\omega}{3\hbar c}|\vec{\mu}_{ba}|^2 \times \sum_{v}\sum_{v'} P_{av}\,|\langle\Theta_{bv'} \mid \Theta_{av}\rangle|^2 D(\omega_{bv',av}+\omega), \tag{1}$$

in which $|\langle\Theta_{bv'} \mid \Theta_{av}\rangle|^2$ is the Franck–Condon factor, $\vec{\mu}_{ba}$denotes the electronic transition dipole moment, P_{av} the Boltzmann factor, and c the speed of light. $D(\omega_{bv',av}+\omega)$ in Eq. (1) is the Lorentzian line-shape function. If we use the displaced harmonic oscillator approximation plus the first-order anharmonic correction, Eq. (1) can be reduced as[29]

$$I(\omega) = \frac{2\pi\omega}{3\hbar}|\vec{\mu}_{ba}|^2\int_{-\infty}^{\infty} dt\, e^{-it(|\omega_{ba}|+\Omega_0-\omega)-\gamma_{ba}|t|} \times\exp\Big[-\sum_j S_j(1-3\eta_j)\{2\bar{v}_j+1 - (\bar{v}_j+1)e^{it\omega_j}-\bar{v}_j e^{-it\omega_j}\}\Big], \tag{2}$$

where $\omega_{ba} = (E_b - E_a)/\hbar$ denotes the electronic adiabatic energy gap and $E_b(E_a)$ stands for the electronic energy at the equilibrium geometry of the state $b(a)$, γ_{ba} represents the dephasing (or damping) width, $\bar{v}_i = (e^{\hbar\omega_i/kT}-1)^{-1}$ is the phonon distribution, and S_i denotes the Huang–Rhys factor

$$S_i = \frac{\omega_i}{2\hbar}d_i^2, \tag{3}$$

in which ω_i is the harmonic frequencies of the ith normal mode. In this case, the displacement d_i in Eq. (3) can be simply calculated by

$$d_i = Q_i' - Q_i = \sum_j L_{ij}(q_j' - q_j), \tag{4}$$

where $q_j'(q_j)$ are the mass-weighted Cartesian coordinates at the equilibrium geometry of the electronic state b (a), and the transformation matrix $\mathbf{L}$ in Eq. (4), along with $q_j'(q_j)$, were calculated using GAUSSIAN 09 program.

The most important quantities Ω_0 and $\eta_j$in Eq. (2) stand for the first-order anharmonic correction to Fracnk–Condon factors and given by[29,30]

$$\Omega_0 = -2\sum_j \eta_j S_j\omega_j, \tag{5}$$

$$\eta_j = \frac{2K_{j3}d_j}{3\omega_j^2}, \tag{6}$$

where K_{j3} is the third derivative of the ground-state potential energy surface with respect to normal mode Q_j that can be calculated by GAUSSIAN 09 program as well. $(1-3\eta_j)S_j$ in Eq. (2) represents the certain effective Huang–Rhys factor that influences profile of fluorescence spectra.

C. Franck–Condon simulation for internal conversion

The internal conversion is due to the breakdown of the Born–Oppenheimer approximation.[31,32] According to the Fermi's golden rule, IC rate constant from initial single vibrational level iv to final f state at temperature $T = 0$ K can be estimated by[33]

$$k_{iv\to f} = \frac{2\pi}{\hbar}\sum_{v'}|\langle\psi_{fv'}|\hat{H}'_{BO}|\psi_{iv}\rangle|D(E_{fv'}-E_{iv}), \tag{7}$$

where $\hat{H}'_{BO}$denotes the nonadiabatic coupling operator. The coupling matrix element is estimated by

$$\langle\psi_{fv'}|\hat{H}'_{BO}|\psi_{iv}\rangle = -\hbar^2\sum_l\langle\Phi_i\Theta_{iv}|\left|\frac{\partial\Phi_f}{\partial Q_l}\frac{\partial\Theta_{fv'}}{\partial Q_l}\right\rangle, \tag{8}$$

where Θ_{iv} and $\Theta_{fv'}$are vibrational wave functions for nuclear motion, Φ_i and Φ_f represent wave functions for electronic motion, and Q_l is the mass-weighted vibrational normal coordinate of the promoting mode. Since we are interesting the IC rate constant from the single vibronic level iv produced by the pumping laser, so that we can use the Condon and the displaced harmonic oscillator approximations under the collision-free condition to simplify Eq. (7) as[34]

$$k_{iv\to f} = \frac{1}{\hbar^2}|R_l(fi)|^2\int_{-\infty}^{\infty} dt\exp\Big[it(\omega_{fi}+\omega_l)-\gamma_{if}|t| - \sum_j{}_j(1-e^{it\omega_j})\Big]\prod_k g_{v_k}(t), \tag{9}$$

where

$$g_{v_k}(t) = \sum_{n_k=0}^{v_k}\frac{v_k!}{(v_k-n_k)!(n_k!)^2}[S_k(e^{it\omega_k/2}-e^{-it\omega_k/2})^2]^{n_k}. \tag{10}$$

In the present work, we only consider $v_k = 0$, and thus $g_{v_k}(t) = 1$. $R_l(fi)$ in Eq. (9) denotes the vibronic coupling for single prompting mode l between the initial and final electronic states and it is given by

$$R_l(fi) = -\hbar^2\sqrt{\frac{\omega_l}{2\hbar}}\langle\Phi_f|\,\partial/\partial Q_l\,|\Phi_i\rangle, \tag{11}$$

TABLE I. The equilibrium geometries of the ground state [$S_0(^1A_1)$] and the first excited state [$S_1(^1B_2)$] optimized by different levels of method for the fluorobenzene. Bond lengths are given in angstroms and bond angles in degrees. All calculations are based on basis set 6-311++G**. The atom numbering is shown in Fig. 1.

Method		C_1F_7	C_1C_2	C_2C_3	C_3C_4	C_2H_8	C_3H_9	C_4H_{10}	$F_7C_1C_2$	$C_6C_1C_2$	$C_1C_2C_3$	$C_2C_3C_4$	$C_3C_4C_5$
TD(B3LYP)	S_0	1.357	1.386	1.394	1.394	1.083	1.084	1.083	118.7	122.6	118.3	120.4	119.8
	S_1	1.342	1.426	1.424	1.424	1.080	1.081	1.083	117.6	124.8	117.2	119.4	122.0
TD(B3LYP-35)	S_0	1.346	1.381	1.389	1.389	1.079	1.080	1.079	118.7	122.5	118.4	120.4	119.8
	S_1	1.331	1.410	1.417	1.419	1.076	1.077	1.079	117.6	124.7	117.3	119.4	122.0
TD(BHandHLYP)	S_0	1.338	1.376	1.385	1.385	1.075	1.076	1.076	118.8	122.5	118.4	120.4	119.8
	S_1	1.322	1.406	1.412	1.415	1.073	1.073	1.076	117.7	124.7	117.3	119.3	122.0
HF/CIS	S_0	1.328	1.377	1.386	1.386	1.074	1.075	1.075	118.8	122.4	118.4	120.5	119.7
	S_1	1.312	1.406	1.410	1.415	1.072	1.072	1.074	117.9	124.2	117.6	119.5	121.5
RICC2[a]	S_0	1.349	1.386	1.393	1.393	1.078	1.079	1.079	118.8	122.4	118.5	120.5	119.8
	S_1	1.339	1.419	1.428	1.428	1.076	1.077	1.079	117.6	124.8	117.3	119.3	122.0
Expt.[b]	S_0	1.355	1.382	1.395	1.395	1.077	1.078	1.077	118.5	123.1	118.1	120.5	119.8

[a]See Ref. 5.
[b]See Ref. 9.

where the electronic nonadiabatic coupling matrix elements $\langle \Phi_f | \partial / \partial Q_l | \Phi_i \rangle$ were computed by the MOLPRO program.[24] For simplicity, the term $\frac{1}{\hbar^2} |R_l(fi)|^2$ in Eq. (9) is called as the electronic part of the IC rate constant. The integration part in Eq. (9) is the Franck–Condon factor basically same as the corresponding integration part in Eq. (2) for fluorescence emission spectra without including anharmonic correction. Therefore, accuracy of spectral calculation can directly reflect accuracy of internal conversion calculation. In the present work, we consider the calculation of IC rate constant from the single vibronic levels of the first singlet excited state S_1 to the ground state S_0.

III. RESULTS AND DISCUSSIONS

A. Equilibrium geometries and vibrational frequencies

The geometrical optimizations were carried out using DFT and HF methods for electronic ground state, and TDDFT and CIS methods for the first excited state. In fact, the structural optimizations of FB have been performed using a set of *ab initio* methods and the results have been analyzed in more detail.[4,5] We presented our calculation results and made a comparison with other theoretical calculation[5] as well as available experimental data.[9] Optimized geometrical parameters are given in Table I with the atom numbering scheme adopted in Fig. 1. Table I shows that for the geometries of both S_0 and S_1 states all the geometrical parameters calculated from the three functionals (B3LYP, B3LYP-35, and BHandHLYP) agree well each other and also agree with Ref. 5's calculations, and all of them agree with experiment observation in reasonable accuracy. For example, for the ground state S_0, the C_1F_7 bond length is 1.357 (from B3LYP) and 1.346 (from B3LYP-35) in comparison with experiment value 1.355, $C_6C_1C_2$ bond angle is 122.6 (from B3LYP) and 122.5 (from B3LYP-35) in comparison with experiment value 123.1. The other geometry parameters calculated from B3LYP and B3LYP-35 show even smaller discrepancies in comparison with the corresponding experiment values. Overall, the geometry parameters calculated from the B3LYP show closer to the experimental values than those of the B3LYP and BHandHLYP calculations. Moreover, we did HF/CIS calculation for the geometrical optimizations, and its results shown in Table I are very similar to the results calculated from BHandHLYP functional.

Calculated vibrational frequencies of S_0 and S_1 states are displayed in Table II in comparison with other theoretical calculations and available experimental data. It should be noted that frequency calculations are used not only for simulating fluorescence spectra but also for verifying optimized equilibrium geometries as true minima for the two electronic states involved in the transition. Table II shows that vibrational frequencies simulated with the three functionals (B3LYP, B3LYP-35, and BHandHLYP) are in very good agreement with the experimental observations[2,4,6] as well as the other theoretical calculations[4,5] for both electronic ground S_0 and the first excited S_1 states, and this indicates that the calculated frequencies can be used directly to simulate the fluorescence spectra without scaling. For example, the frequencies calculated from B3LYP method are just scaled by a factor of 0.98 to reproduce the experimental values very well (see Table II). However, vibrational frequencies simulated from HF and CIS methods are much larger than the corresponding experimental values. It should be pointed out that in the present calculation the normal mode ν_{10} is assigned as the closest analogy to the ring-breathing mode in benzene molecule.[36] This is different from Ref. 4 where it is normal mode ν_8. In the present work we chose the Mulliken notation to label the vibrations of FB molecule and the corresponding Wilson notation only quoted in the tables.

In order to confirm that the displaced harmonic oscillator approximation is good approximation to be used for simulating the DF electronic spectrum as well as IC rate constant, it requires that difference between vibrational frequencies of S_0 and S_1 states must be small for each of the eleven totally symmetry vibrational normal modes (a_1-type). Table II shows that for example, the frequencies of the mode ν_{10} for the S_0 and S_1 states are 819 and 793 cm^{-1} (from B3LYP calculations), respectively, and its difference is just 26 cm^{-1}. This difference is just 8 cm^{-1} from B3LYP-35 method and 24 cm^{-1} from BHandHLYP method.

TABLE II. Calculated and experimental vibrational frequencies (cm^{-1}) of fluorobenzene for the $S_0(^1A_1)$ and $S_1(^1B_2)$ states.

		S_0							S_1						
Sym	Mode[a]	B3[b]	B35[c]	BH[d]	HF	calc.[e]	Expt.[f]	Expt.[g]	B3[b]	B35[c]	BH[d]	CIS	calc.[e]	Expt.[f]	Expt.[g]
a_1	1(20a)	3203(3139)	3218	3298	3362	3242	3094	…	3230	3282	3325	3390	3262	…	…
	2(2)	3191(3128)	3207	3287	3350	3232	3080	…	3214	3266	3310	3374	3246	…	…
	3(13)	3170(3107)	3186	3265	3325	3210	3061	…	3187	3240	3284	3351	3221	…	…
	4(8a)	1634(1601)	1624	1715	1785	1632	1605	…	1560	1608	1648	1720	1547	…	…
	5(19a)	1522(1491)	1501	1587	1652	1520	1500	…	1448	1483	1513	1581	1431	…	…
	6(7a)	1234(1210)	1246	1301	1357	1252	1238	1239	1236	1275	1307	1363	1244	1220	1230
	7(9a)	1175(1151)	1144	1216	1262	1177	1156	1156	1150	1173	1192	1240	1144	922	…
	8(18a)	1038(1018)	1025	1076	1109	1036	1023	1023	988	1009	1028	1067	936	916	917
	9(1)	1018(998)	1008	1054	1083	1014	1009	1009	959	983	1003	1037	978	968	969
	10(12)	819(802)	820	853	879	818	809	810	793	812	829	855	780	765	765
	11(6a)	524(514)	515	543	561	517	517	517	472	480	488	505	459	460	460
a_2	12(17a)	965(946)	888	1022	1088	923	957	957	617	650	678	759	597	…	643
	13(10a)	828(812)	747	873	927	839	818	818	484	517	544	631	487	…	509
	14(16a)	421(413)	374	440	460	426	414	413	162	168	166	142	209	206	206
b_1	15(5)	972(952)	895	1029	1095	955	978	978	785	814	840	891	738	…	755
	16(17b)	905(887)	831	955	1010	902	895	895	658	691	719	785	611	…	661
	17(10b)	765(749)	692	803	846	770	754	754	588	613	634	679	571	555	555
	18(4)	677(664)	627	711	747	666	687	687	472	490	505	512	458	…	451
	19(16b)	505(495)	444	530	558	512	498[e]	498	310	321	330	341	334	…	331
	20(11)	237(232)	182	249	263	238	249[e]	233	174	181	186	196	174	182	167
b_2	21(20b)	3201(3137)	3216	3296	3360	3239	…	…	3226	3278	3321	3386	3259	…	…
	22(7b)	3179(3116)	3195	3275	3336	3218	3069	…	3207	3259	3302	3366	3240	…	…
	23(8b)	1643(1610)	1635	1719	1784	1639	1605	…	1523	1554	1615	1824	1531	…	…
	24(19b)	1485(1456)	1460	1544	1603	1480	1460	…	1460	1534	1567	1573	1399	…	…
	25(14)	1344(1317)	1388	1386	1442	1430	1301	…	1421	1455	1485	1537	1691	1589	1589
	26(3)	1325(1298)	1290	1347	1322	1322	…	1250	1301	1328	1351	1397	1284	…	…
	27(9b)	1180(1156)	1146	1211	1200	1178	1128	1128	1170	1191	1209	1245	1162	…	…
	28(15)	1090(1068)	1065	1127	1155	1088	1066	1066	1012	1040	1063	1107	987	976	955
	29(6b)	627(615)	613	649	671	614	614	614	526	534	540	566	514	519	518
	30(18b)	404(396)	381	421	440	402	400	404	392	401	408	427	384	387	388

[a]Mulliken notation and, in parentheses, the Wilson notation are given.
[b]The frequencies in parentheses have been scaled by a factor of 0.98. B3 denotes B3LYP functional.
[c]B35 denotes B3LYP-35 functional.
[d]BH denotes BHandHLYP functional.
[e]Reference 5 (RICC2/def2-TZVPP).
[f]Reference 6.
[g]Reference 4.

B. Electronic structures and excitation energies

We have done calculations of vertical excitation energies and its corresponding oscillator strengths for the first two singlet-excited states estimated at equilibrium geometry of the ground state. Table III shows the vertical excitation energies to S_1 state 5.32, 5.51, and 5.67 eV, respectively, calculated from B3LYP, B3LYP-35, and BHandHLYP functionals and they all overestimate experimental value (4.69 eV),[12] but are better than the previous value (5.81 eV) reported by Padma *et al.*[13] which is just the same as the present CIS calculation. The present calculations showed the more percentage of HF exchange in the functional, the more overestimation of vertical excitation energy to S_1 state. This tendency is consistent with the HF method that does not include the correlation energy. Besides, the present calculation based on the three functionals in text also shows lower adiabatic energy gaps between S_0 and S_1 states than that of Ref. 13. The experimental studies[12,35–39] showed that the substitution of fluorine in benzene does not change the symmetry order of S_1 and S_2 states, and this indicates that the $^1B_2$ corresponds to the first excited state and $^1A_1$ corresponds to the second excited state. The present calculations confirm all the experimental conclusion. On the other hand, the present calculations showed that the first excited state S_1 has a $\pi\pi^*$ transition feature, and thus the significant changes in geometry come from the CC bond lengths when the $^1B_2 \leftarrow {}^1A_1$ transition occurs. The present natural orbital calculation predicted that the S_1 state results mainly from the mixing excitation of the HOMO $\rightarrow$ LUMO (0.71 electron excited) and the HOMO $-$ 1 $\rightarrow$ LUMO $+$ 1 (0.29 electron excited), and its frontier molecular orbitals are depicted in Fig. 2 and this agrees with calculations reported by Pugliesi *et al.*[5] In comparison with experimental vertical excitation energy to S_2 state 6.21 eV, B3LYP-35 and BHandHLYP methods show the best agreement as shown in Table III, while B3LYP method shows the underestimation and CIS method shows the overestimation.

TABLE III. Calculated vertical transition energy (ΔE, unit is eV), adiabatic transition energy gap and oscillator strengths (f) from $S_0(^1A_1)$ to $S_1(^1B_2)$ together with the experimental data and the previous calculations.

		(TD)B3LYP		(TD)BHandHLYP		(TD)B3LYP-35		HF/CIS		calc.	Expt.[a]	
State	Sym	ΔE[b]	f	ΔE[b]	f	ΔE[b]	f	ΔE[b]	f	ΔE[b]	ΔE	f
S1	B2	5.32 (5.18)	0.013	5.67 (5.53)	0.016	5.51 (5.37)	0.015	6.16 (6.02)	0.019	5.81[c] (5.78)	4.69	0.007
S2	A1	6.05	0.000	6.23	0.000	6.17	0.000	6.37	0.002	6.55[c]	6.21	0.081

[a]Reference 12.
[b]The adiabatic energies are given in parentheses.
[c]Reference 13, the used method was SINDO1.
[d]Basis set 6-311++G** is used for all the present calculations.

Let us now turn to discuss oscillator strengths of excitation transitions vertically from the ground state to excited states. Relative strengths measured from experiment[12] are 0.007 and 0.081 for excitation to S_1 and S_2 states, respectively, as shown in Table III. The present calculations do not reproduce this order of excitation strengths.

C. Franck–Condon simulation of the DF spectrum

The dispersed fluorescence spectrum of the $A\ ^1B_2 \rightarrow X\ ^1A_1$ transition was measured and the detailed analyses were reported in the recent experiment studies,[4] where the DF spectral profile is primarily described by the Franck–Condon progression in terms of the totally symmetry normal modes (a_1-type). Among these modes, ν_9 and ν_{10} are the main progression forming modes in the $^1B_2 \rightarrow {}^1A_1$ fluorescence spectrum. The present calculations confirmed that modes ν_{10} and ν_9 have the largest Huang–Rhys factors ($S = 0.420$ and 0.408 for instance from B3LYP calculation as shown in Table IV) and are assigned as the closest analogy to the ring-breathing modes in benzene as shown in Fig. 3. This differs from Ref. 4 in which ν_4 and ν_9 were interpreted as the ring-breathing modes. The modes ν_2, ν_3, ν_4, and ν_5, which are relative to the CH stretching and bending vibrations, have little contribution to FC factor as their Huang–Rhys factors are negligible small. Furthermore, the previous theoretical analysis[4,5] also indicated that there exist very weak bands in the DF spectrum, most of them are related to the nontotally symmetric normal modes, e.g., ν_{19} and ν_{16} (b_1 symmetry), that can be interpreted in terms of Duschinsky mixing.

In the present spectrum simulation, we utilized the unscaled vibrational frequencies calculated at the same levels of *ab initio* method as was performed for optimizing the geometries of the electronic states in Sec. III A. The band origin (0–0 transition) is set up to be zero (cm^{-1}) in the DF spectrum as it was adopted in experimental study.[4] In order to simulate the experimental resolution of the DF spectrum, Lorentzian broadening width in Eq. (2) is tested as $\gamma_{ab} = 10\ cm^{-1}$ approximately. We know that this value contains not only the truly dephasing but also the contribution from the

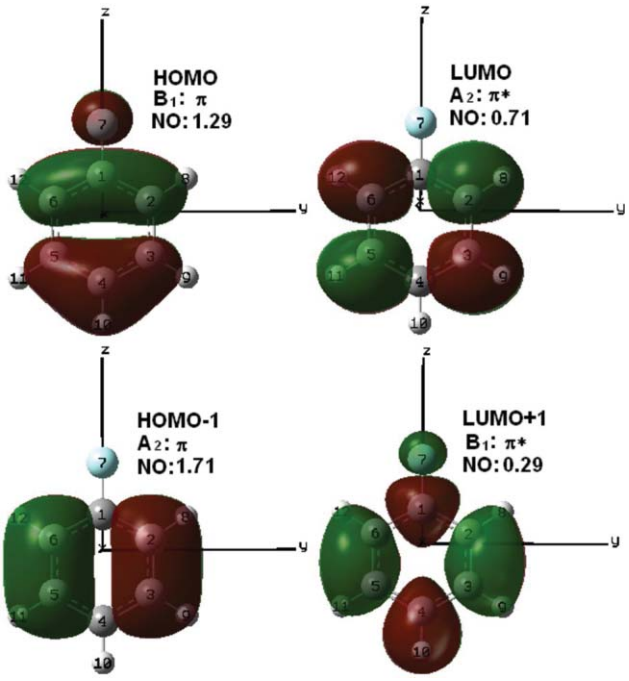

FIG. 2. The selected frontier molecular orbitals of fluorobenzene.

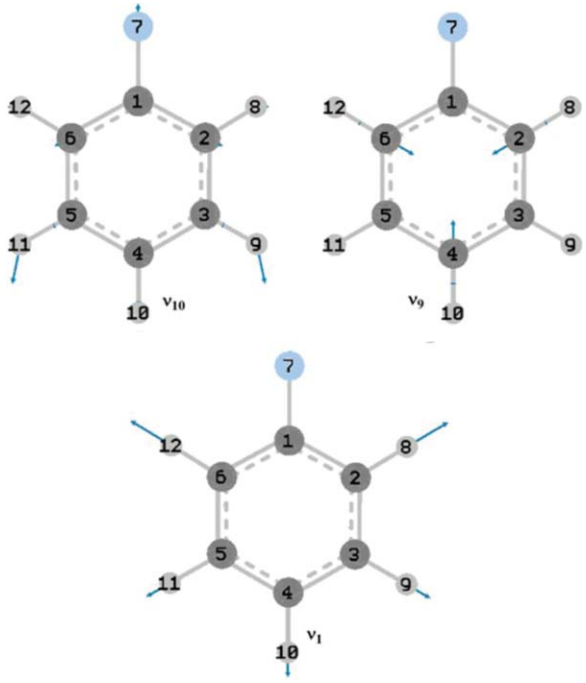

FIG. 3. The displacement vector of the three vibrational modes ν_{10}, ν_9, and ν_1.

TABLE IV. Calculated vibrational frequencies (Freq., in cm $^{-1}$), cubic force constant (K_j3, in hartree * amu$^{-3/2}$ * bohr^{-3}) of the diagonal elements of $S_0(^1A_1)$ state, Huang–Rhys factors [S(s1)], Franck–Condon factors in the displaced oscillator approximation (FC_{disp}) and in the distorted oscillator approximation (FC_{dist}) (Value smaller than 0.0002 was neglected), and anharmonic parameters (η_j) for $S-1(^1B_2)$.

	$S_0(^1A_1)$				$S_1(^1B_2)$							
	B3LYP		HF		TD(B3LYP)				CIS			
Mode[a]	Freq.	K_j3	Freq.	K_j3	S(s1)	FC_{disp}[b]	FC_{dist}[c]	$\eta_j/2$	S(s1)	FC_{disp}[b]	FC_{dist}[c]	$\eta_j/2$
1(20a)	3203	−0.605	3362	−0.625	0.223	0.1784	0.0000	−0.140	0.1905	0.1574	0.0000	−0.120
2(2)	3191	0.433	3350	0.376	0.001	0.0009	0.0000	−0.006	0.0006	0.0006	0.0000	−0.004
3(13)	3170	−0.117	3325	−0.081	0.027	0.0263	0.0000	−0.009	0.0216	0.0212	0.0000	−0.005
4(8a)	1634	−0.030	1785	−0.031	0.002	0.0020	0.0000	−0.004	0.0054	0.0054	0.0000	−0.005
5(19a)	1522	0.003	1652	0.004	0.001	0.0009	0.0000	−0.000	0.0016	0.0016	0.0000	−0.000
6(7a)	1234	0.021	1357	0.031	0.085	0.0780	0.0000	0.032	0.0584	0.0551	0.0000	0.0301
7(9a)	1175	−0.004	1262	−0.004	0.006	0.0056	0.0000	−0.002	0.0047	0.0047	0.0000	−0.002
8(18a)	1038	−0.005	1109	−0.004	0.017	0.0168	0.0000	−0.005	0.0120	0.0119	0.0000	0.0025
9(1)	1018	0.005	1083	0.006	0.408	0.2712	0.0000	−0.025	0.3568	0.2497	0.0000	−0.026
10(12)	819	−0.005	879	−0.006	0.420	0.2758	0.0000	−0.050	0.3631	0.2525	0.0000	−0.041
11(6a)	524	−0.001	561	−0.001	0.154	0.1323	0.0000	−0.010	0.1293	0.1136	0.0000	−0.008
12(17a)	965	0.000	1088	0.000	0.000	0.0000	0.0236	0.000	0.0000	0.0000	0.0156	0.0000
13(10a)	828	0.000	927	0.000	0.000	0.0000	0.0333	0.000	0.0000	0.0000	0.0177	0.0000
14(16a)	421	0.000	460	0.000	0.000	0.0000	0.0883	0.000	0.0000	0.0000	0.1183	0.0000
15(5)	972	0.000	1095	0.000	0.000	0.0000	0.0056	0.000	0.0000	0.0000	0.0053	0.0000
16(17b)	905	0.000	1010	0.000	0.000	0.0000	0.0123	0.000	0.0000	0.0000	0.0078	0.0000
17(10b)	765	0.000	846	0.000	0.000	0.0000	0.0085	0.000	0.0000	0.0000	0.0060	0.0000
18(4)	677	0.000	747	0.000	0.000	0.0000	0.0157	0.000	0.0000	0.0000	0.0171	0.0000
19(16b)	505	0.000	558	0.000	0.000	0.0000	0.0277	0.000	0.0000	0.0000	0.0283	0.0000
20(11)	237	0.000	263	0.000	0.000	0.0000	0.0117	0.000	0.0000	0.0000	0.0105	0.0000
28(15)	1090	0.000	1155	0.000	0.000	0.0000	0.0007	0.000	0.0000	0.0000	0.0002	0.0000
29(6b)	627	0.000	671	0.000	0.000	0.0000	0.0038	0.000	0.0000	0.0000	0.0036	0.0000

[a]Mulliken notation, the Wilson notation are given in parentheses.
[b]For the displaced approximation, only the Franck–Condon factors of 0–1 transitions are given.
[c]The data from 0–2 transitions in the distorted oscillator approximation.

instrumental broadening. The DF spectrum simulated from B3LYP, B3LYP-35, BHandHLYP, and CIS methods all show that the 0–0 transition is the strongest transition in the allowed $^1B_2 \rightarrow {}^1A_1$ electronic transition as shown in Figs. 4 and 5, and this agrees with experiment observation. All simulated DF spectra in Figs. 4 and 5 were performed in the framework of displaced harmonic and anharmonic oscillator approximation, respectively, in which the most prominent peaks have been assigned based on the present calculations in comparison with experimental data. It can be seen that all methods including CIS reproduce qualitatively the essential character of the observed spectrum.

According to the high resolution of experimental results performed by Butler *et al.*,[4] the DF spectrum is mostly assigned as the totally symmetric normal mode progressions; especially the mode ν_9 displays very strong intensity in the spectral profile and in the present B3LYP calculation the intensity of the vibronic line assigned as 9_1^0 fundamental [see Fig. 3(b)] is slightly underestimated; the intensity of 9_1^0 transition in experiment is about 70% of that of the 0–0 line, but that in the present calculation is about 50%. Harmonic Franck–Condon simulations in Fig. 4 indicate that the strongest and second strongest vibronic transitions are the 10_1^0 and 9_1^0 (after the 0–0 transition) which seems to be reversed in comparison with the experiment result. When anhramonic corrections are added, simulations in Fig. 5 from all methods except B3LYP-35 show that the 9_1^0 band is larger than 10_1^0 band in good agreement with experimental observation. Moreover, Harmonic Franck–Condon simulations in Fig. 4 indicate that there is strong peak in high energy region of DF spectra and this corresponds to 1_1^0 transition. When anharmonic corrections are added, simulations in Fig. 5 from all methods show that 1_1^0 transition is diminished. This is because that Huang–Rhys factor 0.22 for mode ν_1 is significantly reduced with anharmonic correction as shown in Table IV. Within harmonic approximation vibrational displacement vector for mode ν_1 (CH stretching) is very large as shown in Fig. 3 and even if CH bond lengths change very small from S_0 to S_1 state, Huang–Rhys factor is still as big as 0.22. However, anharmonic correction is also large as shown in Table IV and it effectively cancels out 1_1^0 transition. We can conclude that the amount of HF exchange (from 20% in B3LYP, 35% in B3LYP-35, 50% in BHandHLYP, and 100% in HF) does impact the geometries and vibrational frequencies of FB molecule, but not the relative intensities of the transitions. It is anharmonic corrections that influence the relative intensities of the transitions.

The experimental spectra in Figs. 4(a) and 5(a) show that the 10_1^0 transition strongly overlaps with 14_2^0 transition with a just split 15 cm^{-1}. According to the calculations based on the nontotally symmetric vibrational transitions (see Table IV), it is found that the 14_2^0 should be about one-third of the 10_1^0 in transition intensity. It should be also noticed that

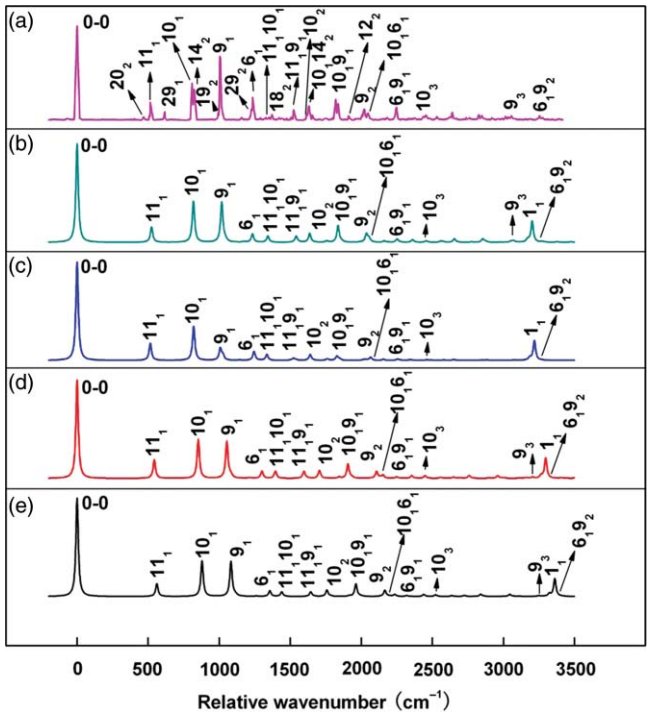

FIG. 4. The DF spectra of fluorobenzene from S_1 to S_0 transition calculated by harmonic FC simulation (the relative energy of the 0–0 transition is set up to be zero). (a) Experimental result from Ref. 4. (b) (TD) B3LYP, (c) (TD) B3LYP-35, (d) (TD)BHandHLYP, and (e) HF/CIS calculations.

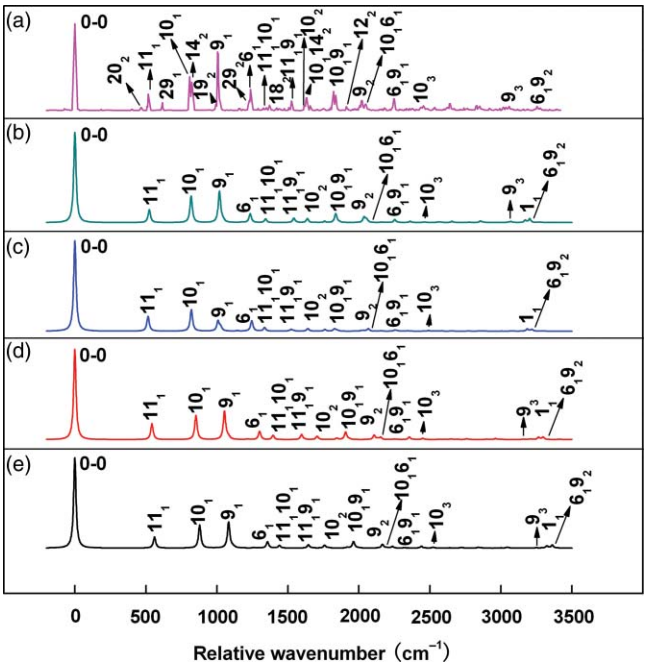

FIG. 5. The same as Fig. 4 but including anharmonic corrections.

in the present simulation, the 10_2^0 transition and the combination band $10_1^0 14_2^0$ are nearly degenerate vibronic level pairs; the vibrational origins of 10_2^0 ($2\nu_{10} = 1637$ cm^{-1}) and $10_1^0 14_2^0$ ($\nu_{10} + 2\nu_{14} = 1613$ cm^{-1}) are separated by 24 cm^{-1} from B3LYP calculation. This suggests that there should be strong coupling between these two vibronic transitions (ν_1 and ν_{14}). On the other hand, from B3LYP calculation as shown in Figs. 4(b) and 5(b) we could assign the 10_2^0 (1637 cm^{-1}, that is, $2\nu_{10}$), 10_3^0 (2456 cm^{-1}), 9_2^0 (2036 cm^{-1}), and 9_3^0 (3054 cm^{-1}) vibronic transitions as four fundamentals located at 1613, 2434, 2016, and 3014 cm^{-1} in experiment,[4], respectively. The detailed assignments based on the present analysis are shown in very good agreement with the experimental data as displayed in Table V. In the low energy region of the DF spectrum, the experimental observation and the present B3LYP simulation agree well for the significant intensity assigned from normal mode ν_{11}, and this corresponds to Huang–Rhys factor $S = 0.154$ (from B3LYP) as shown in Table IV. Intensity of 6_1^0 band in the harmonic Franck–Condon simulation is lower than corresponding experiment intensity, but it is improved with anharmonic correction as shown in Fig. 5. This fundamental ν_6 corresponds to the CF bond stretching in the present analysis. Furthermore, the experimental DF spectrum reported by Butler *et al.*[4] showed that there are many moderate intensity peaks with the characteristics of combination between fundamental modes. Most of these transitions can be assigned based the present FC simulations. Figures 4(a) and 4(b) [Figs. 5(a) and 5(b)] show very good agreement between experimental result and the present B3LYP simulation for the DF spectrum in terms of the ordering and positioning of these combination peaks and its intensity strengths, especially for extremely weak peak of the combination band of $9_2^0 6_1^0$ in the high frequency region.

Another issue is related with how nontotally symmetry modes contribute to the DF spectrum. As we know that a large number of overtones of out-of-plane vibrations were described and interpreted as contribution from the nontotally symmetric vibrational modes in the experimental DF spectrum.[4] For example, the transitions involving the a_2 and b_1 vibrations,14_2^0, 19_2^0, and 18_2^0, have relative moderate intensities which cannot included in the simulation with displaced oscillator approximation. In order to include contributions from the nontotally symmetric vibrational transitions, we must use the distorted harmonic oscillator approximation.[28] The distorted effect from the change of frequency between the ground and excited states is generally small, but it can be observed experimentally when the ratio between $|\omega_g - \omega_e|$ and $|\omega_g + \omega_e|$ (ω_g and ω_e are the vibrational frequencies of the ground state and the excited state) is large for the mode involved in the electronic excitation. As shown in Table II, based on the present calculations some of the out-of-plane vibrations have a large change in frequencies. For example, for the mode ν_{12} with a_2 symmetry, the frequency difference between S_0 and S_1 states is 348 cm^{-1} (from B3LYP) and in this case the distorted effect should be considered.

According to Eq. (1), the fluorescence coefficient $I(\omega)$ is proportional to the Franck–Condon factor. Within the displaced approximation, the Franck–Condon factor can be derived as[27,28]

$$F_{\nu_i'} = \left|\left\langle \Theta_{b\nu_i'} \middle| \Theta_{a0_i} \right\rangle\right|^2 = \frac{S_i^{\nu_i'}}{\nu_i'!} e^{-S_i}, \tag{12}$$

where v_i' denotes the vibrational quantum number of the ith normal mode and S_i is the Huang–Rhys factor. Similarly, the Franck–Condon factor in the distorted harmonic approximation is given by[27,28]

$$F_{v_i'} = |\langle \Theta_{bv_i'} | \Theta_{a0_i} \rangle|^2 = \frac{\sqrt{\omega_i \omega_i'}}{\omega_i + \omega_i'} \left(\frac{\omega_i' - \omega_i}{\omega_i' + \omega_i} \right)^{v_i'} \frac{v_i'!}{2^{v_i'-1}[(v_i'/2)!]^2}, \quad (13)$$

where v_i' can be only taken as an even integer number, ω_i and ω_i' correspond to vibrational frequencies for different electronic states. We can see that, unless $\omega_i' \gg \omega_i$ (or $\omega_i' \ll \omega_i$), $F_{v_i'}$ is much smaller than unity. By applying Eqs. (12) and (13), we have computed the displaced Franck–Condon factors of 0–1 transitions and the distorted ones of 0–2 transitions for all 30 vibrational modes and their values are listed in Table IV. Generally, the intensities of 0–2 transitions (overtones) of the out-of-plane modes are very small. For example, the largest distorted Franck–Condon factor arises from transition of 14_2^0 is only 0.0883 based on the B3LYP calculation. Using the displaced–distorted approximation with adding distorted FC factors of Eq. (13) into Eq. (1), we simulated the DF spectrum of the $^1B_2 \rightarrow {}^1A_1$ electronic transition again. Figure 6(b) displays the spectrum simulated from B3LYP method in comparison with experiment result given in Fig. 6(a). It can be seen that most of the overtones are reproduced correctly. For example, the line at 474 cm^{-1} is assigned as the 20_2^0 transition, which agrees well with the transition at 466 cm^{-1} assigned experimentally. Furthermore, the predicted band positions of overtones 14_2^0, 18_2^0, and 12_2^0 show an excellent agreement with the experiment. In the present calculations, the transitions of 19_2^0 and 9_1^0, 29_2^0 and 6_1^0 appear at almost the same positions (that is, $19_2^0 = 1010\ cm^{-1} \approx 9_1^0 = 1018\ cm^{-1}$ and $29_2^0 = 1254\ cm^{-1} \approx 6_1^0 = 1234\ cm^{-1}$). It is should be noted that the intensities of these out-of-plane vibrations are enlarged due to their notably distorted Huang–Rhys factors. However, the 0–1 transition of mode v_{29} with b_2-type symmetry is still not reproduced by the present displaced–distorted calculation. This kind of the vibrational transition is induced by the Herzberg–Teller effect, which is not included in the present FC simulation.

D. Internal conversion and the lifetime of S_1 state

In order to compute internal conversion constant, we have to compute the nonadiabatic coupling matrix elements or vibronic couplings $\langle \Phi_f | \partial / \partial Q_l | \Phi_i \rangle$ (between S_0 and S_1 states) vertically at equilibrium geometry of S_1 state. At the equilibrium geometry of S_1 state calculated by two methods; (TD)B3LYP and HF/CIS, we employed CASSCF method for calculating nonadiabatic coupling matrix elements. We should mention that the equilibrium geometry optimized by (TD)B3LYP and HF/CIS methods may or may not correspond to true equilibrium optimized by CASSCF method, but on the other hand, vibronic couplings vary very slowly against change of geometry. We first computed vibronic couplings in Cartesian coordinate spaces and then transformed them into normal mode coordinates. However, we have to lowering group symmetry to C_1 in order to perform vibronic couplings by MOLPRO. We obtained 30 vibronic couplings

TABLE V. Theoretical frequencies and assignments of transitions in the DF spectrum using the displaced oscillator approximation. The relative energies of the origin bands in both experimental and theoretical spectra are set up to be zero. The experimental data is taken from Ref. 4.

Assignment[a]	Expt.[d]	B3LYP[b]	B35	BH	HF/CIS
20_2 (11_2) [c]	466				
11_1 ($6a_1$)	519	524(514)	515	543	561
29_1 ($6b_1$)	611				
10_1 (12_1)	810	819(802)	820	853	879
14_2 ($16a_2$)	826				
9_1 (1_1)	1008	1018(998)	1008	1054	1083
6_1 ($7a_1$)	1239	1234(1210)	1246	1301	1357
11_110_1 ($6a_112_1$)	1326	1343(1316)	1335	1396	1440
18_2 (4_2)	1369				
11_19_1 ($6a_11_1$)	1523	1542(1512)	1523	1597	1644
10_2, or 10_114_2 (12_2 ,or 12_116a_2)	1613	1637(1604)	1640	1706	1758
10_19_1 (12_11_1)	1917	1837(1800)	1828	1907	1962
12_2 ($17a_2$)	1912				
9_2 (1_2)	2016	2036(1996)	2016	2108	2166
10_16_1, or 8_2 (12_17a_1, or $18a_2$)	2045	2053(2012)	2066	2154	2236
6_19_1 ($7a_11_1$)	2243	2252(2208)	2254	2355	2440
10_3 (12_3)	2434	2456(2407)	2460	2559	2637
9_3 (1_3)	3014	3054(2996)	3024	3162	3249
1_1 ($20a_1$)		3203(3139)	3218	3298	3362
9_26_1 (1_27a_1)	3251	3270(3206)	3262	3409	3523

[a]Mulliken notation, the Wilson notation are given in parentheses.
[b]The scaled frequencies by a factor of 0.98 are listed in parentheses.
[c]The subscript n (n = 1, 2, 3) denotes the transition level in the DF spectrum. For example, 20_2 indicates the 0→2 transition involving in the 20 mode.
[d]Reference 4.

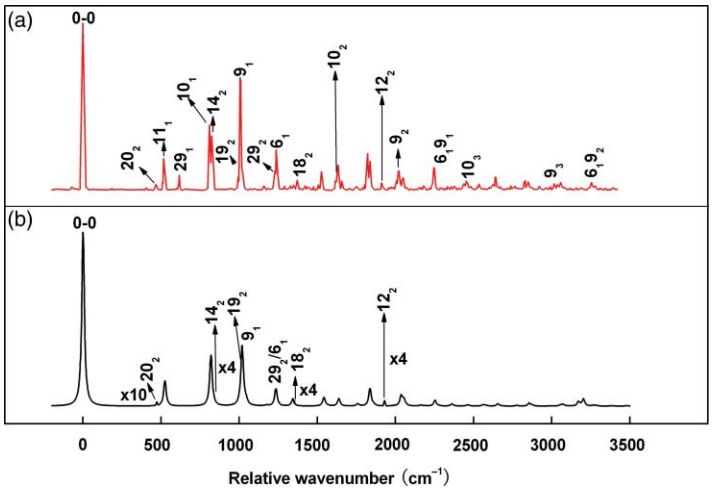

FIG. 6. The same as in Fig. 5 but including distorted effect. (a) Experimental result from Ref. 4. (b) Simulated results with B3LYP calculation in which the intensity of overtone 20_2^0 is enlarged by a factor of 10 and the other overtones are enlarged by a factor of 4.

among which there are only three modes at the same order of magnitude and the rest of them are negligibly small. These three modes do not have clear correspondence to modes obtained with C_{2v} group symmetry. Therefore, we can only label them according to order of frequency magnitude in C_1 symmetry, and they are 7th, 8th, and 15th vibrational normal modes computed by CASSCF. Then, three vibronic couplings are converted to the electronic part of the IC rate $\frac{1}{\hbar^2}|R_l(fi)|^2$ by Eq. (11) and the results are given in Table VI. Two methods produce almost same the coupling matrix elements and its electronic part of the IC rate (see the coupling elements of the 7th normal mode are about 0.1482 and 0.1460 a.u., respectively, from (TD) B3LYP and HF/CIS methods given in Table VI). This is because the optimized geometries of the excited state S_1 performed by two methods show small discrepancies (see Table I), besides vibronic couplings vary slowly against change of geometry. .

Now we turn to compute the second part of IC rate of the transition $^1B_2 \rightarrow {}^1A_1$, and that is the integral part in Eq. (9). The dephasing width γ_{if} in Eq. (9) is chosen as four values; 5 cm^{-1}, 10 cm^{-1}, 15 cm^{-1} and 20 cm^{-1}, so that calculated IC rate $k_{iv\rightarrow f}$ [or lifetime $\tau_l = 1/k_{iv\rightarrow f}\,(l)$] for single promoting mode l is function of dephasing width. Then, we can estimate total lifetime as

$$\tau_T = \frac{1}{\sum_l k_{iv\rightarrow f}\,(l)} = \frac{1}{\sum_l (1/\tau_l)}, \qquad (14)$$

where summation is over three promoting modes (7th, 8th, and 15th in C_1 group symmetry). All results are given in Table VII. Table VII shows that calculated IC rate constants (the lifetimes) increase (decrease) with the increase of the dephasing width for each of the three promoting modes. For example, the TD(B3LYP) calculation indicates that the IC rate constant of mode 8th increases from 2.33×10^7 to 4.23×10^7 s^{-1} when dephasing width increases from 5 to 10 cm^{-1}. It should be emphasized that the electronic part of IC rate $\frac{1}{\hbar^2}|R_l(fi)|^2$ is independent to dephasing width, and thus it is nuclear part of IC rate that is depending on dephasing width. How to determine dephasing width seems becoming a problem. If we use consistent choice of dephasing width for both calculations of the DF spectrum and IC rate, we should choose the dephasing width as 10 cm^{-1} that was used for the DF spectrum simulation in Sec. III C. At $\gamma_{if} = 10$ cm^{-1}, the calculated total lifetimes of the decay $^1B_2 \rightarrow {}^1A_1$ are 11 and 19 ns, respectively, from TD(B3LYP) and HF/CIS calculations in comparison with the experimental value 14.75 ± 0.34 ns (Ref. 16) [the lifetime of 0–0 de-exciting transition is considered so that$g_{v_k}(t) = 1$ in Eq. (9)]. The present calculations show very good agreement with experiment for IC rate constant (or decay lifetime). Taking both the approximations introduced in the present calculations and the experimental uncertainties into consideration, we conclude that the difference between the calculated and the experimental lifetimes (or the IC rates) is quite reasonable. We added anharmonic

TABLE VI. The coupling matrix elements and electronic part of the IC rate of three dominant promoting modes. See detail in context. The Mulliken notation is used to denote the vibrational mode.

		TD(B3LYP)		HF/CIS	
Mode	Sym.	$\langle\Phi_f\|\partial/\partial Q_l\|\Phi_i\rangle$ (a.u.)	$\frac{1}{\hbar^2}\|R_l(fi)\|^2$ ($\times 10^{15}$ cm^{-1}/s)	$\langle\Phi_f\|\partial/\partial Q_l\|\Phi_i\rangle$ (a.u.)	$\frac{1}{\hbar^2}\|R_l(fi)\|^2$ ($\times 10^{15}$ cm^{-1}/s)
7th	a	0.1482	1.1996	0.1460	0.9352
8th	a	0.1324	3.4187	0.1284	2.6908
15th	a	0.1054	2.8348	0.1035	2.3069

TABLE VII. The evaluated IC rate (k_{iv}) and lifetime (τ_1) for each of three promoting modes as well as the total lifetimes (τ_T) for the $^1B_2 \rightarrow {}^1A_1$ transition against different dephasing widths.

		TD(B3LYP)[a]			HF/CIS[a]			Expt.[b]
γ(cm^{-1})	Mode	k_{iv}(10^7 s^{-1})	τ_1(ns)	τ_T(ns)	k_{iv}(10^7 s^{-1})	τ_l(ns)	τ_T(ns)	τ_T(ns)
5	7th	0.65	154	21	0.50	200	44	14.75 ± 0.34
	8th	2.33	43		0.85	118		
	15th	1.69	59		0.94	106		
10	7th	1.48	68	11	0.84	119	19	
	8th	4.23	24		2.42	41		
	15th	3.54	28		2.10	48		
15	7th	2.21	45	7.3	1.26	79	12	
	8th	6.34	16		3.64	27		
	15th	5.31	19		3.15	32		
20	7th	2.95	34	5.4	1.68	60	9.3	
	8th	8.45	12		4.85	21		
	15th	7.08	14		4.20	24		

[a]The vertical transition energies in Table III are used for the calculations of IC rates.
[b]Reference 16.

corrections to the second part of IC rate, and its results are the same as harmonic approximation.

IV. CONCLUDING REMARKS

In the present studies, we have simulated the DF spectrum and IC rate constant of fluorobenzne following excitation of the $^1B_2(S_1) \leftarrow {}^1A_1(S_0)$ transition from the S_1 state to S_0 state by using displaced harmonic oscillator approximation with and without including anharmonic and distorted correction. Starting from optimization of equilibrium geometries and the corresponding normal mode frequencies of S_0 and S_1 states, we obtained geometry parameters and frequencies generally in good agreement with experimental results[2,4,6] and the previous theoretical calculations.[5] Three kinds of functionals (B3LYP, B3LYP-35, and BHandHLYP) with (TD)DFT method plus HF/CIS method were adopted for *ab initio* calculations for ground and the first excited states. Based on accurate geometry parameters and frequencies calculated by these methods, we could compute displacement d_i between equilibrium geometries of S_0 and S_1 states and Huang–Rhys factor S_i accurately. Therefore, we are pretty confident about the present simulations on the DF spectrum and IC rate constant. Displaced harmonic oscillator approximation presented very good examinations of the spectral profile and the assignments of the active fundamental normal modes in the DF spectrum of fluorobenzene, and its results basically agree well with the previous assignments studied in the literatures.[1–10] Actually, the present calculations proved that totally symmetry vibrational modes dominate spectral profile and the assignments, especially described by the Franck–Condon progression from the ν_9 and ν_{10} modes and then we could also assign the dominant combination bands with moderate intensities, such as the bands $11_1^0 10_1^0$ and $10_1^0 14_2^0$, and so on. This is in good agreement with the experiment. Anharmonic corrections (which correct only totally symmetry modes) improved harmonic simulations simultaneously for the intensity order of 9_1^0 and 10_1^0 bands and diminishing 1_1^0 transition. Anharmonic corrections also improved the other small bands from the rest of totally symmetry modes. We conclude that the amount of HF exchange (from 20% in B3LYP, 35% in B3LYP-35, 50% in BHandHLYP, and 100% in HF) does impact the geometries and vibrational frequencies of FB molecule, but not the relative intensities of the transitions. It is anharmonic corrections that influence the relative intensities of the transitions.

We considered using the distorted corrections (which only correct nontotally symmetry modes) to explain the overtones of out-of-plane vibrations which arise from the nontotally symmetric vibrational modes. The present calculations indicated that some of small peaks in the DF spectrum are due to contributions from the distorted effect. However, its contributions to spectra are basically small in comparison with totally symmetry modes.

By using the CASSCF method, we calculated the electronic matrix elements of nonadiabatic coupling between the S_0 and S_1 states and then we computed the single vibronic level internal conversion rate of the $^1B_2(S_1) \rightarrow {}^1A_1(S_0)$ transition within the collision-free condition. It was found that the IC rate is sensitive to the dephasing width. Around $\gamma_{if} = 10$ cm^{-1} that is adopted for spectrum simulation, the calculated total lifetimes of this decay are in good agreement with the experimental observation.

ACKNOWLEDGMENTS

R. He would like to thank Postdoctoral Fellowship supported by National Chaio Tung University. L. Yang would like to thank support from visiting graduate program in National Chiao-Tung University. This work is supported by National Science Council of the Republic of China under grant no. 97–2113-M-009–010-MY3. C. Zhu would like to thank the MOE-ATU project of the National Chiao Tung University for support. R. He would like to thank the National Natural Science Foundation of China (no. 20803059) for support. The first two authors contributed equally to the present paper.

[1]D. C. Smith, E. E. Ferguson, R. L. Hudson, and J. R. Nielsen, J. Chem. Phys. **21**, 1475 (1953).
[2]E. D. Lipp and C. J. Seliskar, J. Mol. Spectrosc. **87**, 242 (1981).
[3]E. D. Lipp and C. J. Seliskar, J. Mol. Spectrosc. **87**, 255 (1981).
[4]P. Butler, D. B. Moss, H. Yin, T. W. Schmidt, and S. H. Kable, J. Chem. Phys. **127**, 094303 (2007).
[5]I. Pugliesi, N. M. Tonge, and M. C. R. Cockett, J. Chem. Phys. **129**, 104303 (2008).
[6]E. D. Lipp and C. J. Seliskar, J. Mol. Spectrosc. **73**, 290 (1978).
[7]J. Murakami, K. Kaya, and M. Ito, J. Chem. Phys. **72**, 3263 (1980).
[8]A. Uskola, F. J. Basterretxea, and F. Castaño, Mol. Phys. **99**, 133 (2001).
[9]Z. Kisiel, E. Białkowska-Jaworska, and L. Pszczółkowski, J. Mol. Spectrosc. **232**, 47 (2005).
[10]C. D. Keefe, J. Barrett, and L. L. Jessome, J. Mol. Struct. **734**, 67 (2005).
[11]S. H. Wollman, J. Chem. Phys. **14**, 123 (1946).
[12]J. Philis, A. Bolovinos, G. Andritsopoulos, E. Pantos, and P. Tsekeris, J. Phys. B: At. Mol. Phys. **14**, 3621 (1981).
[13]E. J. P. Malar and K. Jug, J. Phys. Chem. **88**, 3508 (1984).
[14]G. Fogarasi and A. G. Császár, Spectrochim. Acta, Part A **44**, 1067 (1988).
[15]M. Miura, Y. Aoki, and B. Champagne, J. Chem. Phys. **127**, 084103 (2007).
[16]A. S. Abramson, K. G. Spears, and S. A. Rice, J. Chem. Phys. **56**, 2291 (1972).
[17]K. G. Spears and S. A. Rice, J. Chem. Phys. **55**, 5561 (1971).
[18]A. D. Becke, Phys. Rev. A **38**, 3098 (1988).
[19]J. P. Perdew, Phys. Rev. B **33**, 8822 (1986).
[20]C. T. Lee, W. T. Yang, and R. G. Parr, Phys. Rev. B **37**, 785 (1988).
[21]A. D. Becke, J. Chem. Phys. **98**, 5648 (1993).
[22]J. Guthmullera and B. Champagne, J. Chem. Phys. **127**, 164507 (2007).
[23]M. J. Frisch, G. W. Trucks, H. B. Schlegel *et al.*, GAUSSIAN 09, Revisions A.01 and A.02, Gaussian, Inc., Wallingford, CT, 2009.
[24]MOLPRO, a package of *ab initio* programs designed by H.-J. Werner, P. J. Knowles, and R. Lindh *et al.*, version 2006.1.
[25]D. C. Todd, G. R. Fleming, and J. M. Jean, J. Chem. Phys. **97**, 8915 (1992).
[26]S. H. Lin and R. Bersohn, J. Chem. Phys. **44**, 3768 (1966).
[27]H. Eyring, S. H. Lin, and S. M. Lin, *Basic Chemical Kinetics* (Wiley, New York, 1980).
[28]S. H. Lin, C. H. Chang, K. K. Liang, R. Chang, Y. J. Shiu, J. M. Zhang, T. S. Yang, M. Hayashi, and F. C. Hsu, Adv. Chem. Phys. **121**, 1 (2002).
[29]H. Wang, C. Zhu, J. G. Yu, and S. H. Lin, J. Phys. Chem. A **113**, 14407 (2009).
[30]C. Zhu, K. K. Liang, M. Hayashi, and S. H. Lin, Chem. Phys. **358**, 137 (2009).
[31]S. H. Lin and R. Bersohn, J. Chem. Phys. **48**, 2732 (1968).
[32]S. Fischer, J. Chem. Phys. **53**, 3195 (1970).
[33]S. H. Lin, J. Chem. Phys. **44**, 3759 (1966).
[34]S. H. Lin, J. Chem. Phys. **58** 5760 (1973).
[35]E. Pantos, J. Philis, and A. Bolovinos, J. Mol. Spectrosc. **72**, 36 (1978).
[36]H. D. Bist, J. C. D. Brand, and D. R. Williams, J. Mol. Spectrosc. **24**, 413 (1967).
[37]J. Christoffersen, J. M. Hollas, and G. H. Kirby, Mol. Phys. **16**, 441 (1969).
[38]K. Kimura and S. Nagakura, Mol. Phys. **9**, 117 (1965).
[39]A. Bolovinos, J. Philis, E. Pantos, P. Tsekeris, and G. Andritsopoulos, J. Mol. Spectrosc. **94**, 55 (1982).